Desalination and Water Treatment
www.deswater.com
doi: 10.1080/19443994.2014.943057

53 (2015) 1450–1459
February

Taylor & Francis
Taylor & Francis Group

The potential roles of granular activated carbon in anaerobic fluidized membrane bioreactors: effect on membrane fouling and membrane integrity

Bing Wu[a], Philip Chuen Yung Wong[a,b], Anthony G. Fane[a,b,*]

[a]*Singapore Membrane Technology Centre, Nanyang Technological University, Cleantech Loop, CleanTech One #06-08, Singapore 637141, Singapore, Tel. +65 67905272; Fax: +65 67910756; email: agfane@ntu.edu.sg (A.G. Fane)*
[b]*School of Civil and Environmental Engineering, Nanyang Technological University, 50 Nanyang Avenue, Singapore 639798, Singapore*

Received 29 October 2013; Accepted 16 June 2014

ABSTRACT

This study examined the behavior of granular activated carbon (GAC) in a hybrid GAC-microfiltration process, which was used to simulate an anaerobic fluidized membrane bioreactor. GAC can exhibit two major beneficial roles in reducing membrane fouling, namely, (1) GAC scours the membranes to limit the cake layer formation and facilitate cake layer removal; (2) GAC tends to absorb potential foulants to reduce the interaction of foulants with the membranes. However, several detrimental effects of GAC on membrane performance were also observed. For example, (1) GAC appeared to release micro- and nano-scaled fine carbon particles, which can form potential foulants. (2) GAC abrasion can induce partial membrane integrity loss, which was proven by membrane permeability increase and microscopic autopsy. Interestingly, it was found that the GAC size had little influence on the scouring-enhanced filtration performance and scouring-induced membrane damage. The properties of the membrane materials were more important in determining the extent of integrity loss of the membrane after GAC abrasion. A membrane with good elongation properties (e.g. polyvinylidene fluoride) and GAC having a suitable size (i.e. less energy consumption) with good stability (i.e. releasing less fine carbon particles) is recommended for the hybrid fluidized GAC-membrane filtration process.

Keywords: Adsorption; Membrane integrity; Membrane permeability; Membrane surface morphology; Rejection rate; Scouring effect

1. Introduction

Anaerobic membrane reactors (AnMBRs) have received increasing attention recently. Compared with conventional aerobic MBRs, AnMBRs have advantages such as low energy consumption or even energy production, less sludge production, potentially low green gas (CO_2/NOx) emission, production of biogas, and enhancing water and nutrient recycling possibilities [1]. Similar to aerobic MBRs, membrane fouling in AnMBRs is a complex phenomenon and is an important factor that could increase energy consumption.

*Corresponding author.

Presented at the conference Engineering with Membranes—Towards a Sustainable Future (EWM 2013) Saint-Pierre d'Oléron, France, 3–7 September 2013

Typically recirculation of biogas is considered as a fouling control strategy in AnMBRs [1]. An alternative approach using fluidization of granular activated carbon (GAC) particles in AnMBRs has been reported recently as an approach to mitigate membrane fouling [2–4].

The initial work on a novel two-stage anaerobic fluidized membrane bioreactor (AFMBR) using GAC particles (10 × 30 mesh, 115–230 g/L, 90–100% bed expansion) as fluidization media was performed by Kim et al. [2]. These authors demonstrated that the scouring effect of GAC particles along membrane surfaces mainly contributed to the membrane fouling reduction rather than the GAC adsorption capability. According to the inertial lift model in a cross-flow filtration process, the presence of GAC particles in the boundary layer enhances the shear stress at the membrane surface and increases lateral inertial lift velocity (i.e. an increase of shear-induced diffusion) [5]. In addition, the physical interaction of GAC particles with membranes allows them to remove the existing cake layers from the membranes or prevent the foulants further deposition on the membranes [6]. The beneficial effects of added carbon (such as powered activated carbon [PAC]) have also been observed in aerobic MBRs where the PAC was shown to play multiple roles [7].

Unfortunately, there are possible adverse effects of GAC addition. First, GAC may break up microbial flocs or large colloidal aggregates in the reactor, causing an increase in the amount of fine foulants. For example, Huang et al. [5] and Wei et al. [8] employed cylindrical, rigid, and plastic suspended carriers to mitigate cake layer fouling in a MBR. They found that the carriers broke up sludge flocs, causing an increase in the amount of small particles and soluble organic carbon, which accelerated membrane fouling. Second, GAC itself could release fine carbon particles by attrition during fluidization. These smaller size carbon particles may act as potential foulants and cause a decline in membrane filtration performance [9,10]. Third, the direct contact of the scouring agents with membrane surfaces may affect membrane integrity. This is illustrated by Siembida et al. [11] who used SEM and integrity tests to check whether the membrane material was damaged by polypropylene granules added to a MBRs. They found that the granular material left brush marks on the membrane surface, although the membrane function was not affected [11].

To date, the positive roles (i.e. scouring/adsorption effects) of GAC in membrane filtration have been established [5,6]. However, whether GAC properties and behavior could negatively influence membrane integrity and membrane filtration performances has not been clearly illustrated. There is a need to examine the extent of these negative effects and determine how to minimize them in order to achieve stable and better membrane filtration performance in a fluidized GAC membrane process (and similar particle-enhanced membrane process).

This study investigated the potential behavior of GAC particles in the membrane filtration process via bench filtration setups. Specifically, we elucidated: (1) the cake layer removal by GAC scouring by a direct observation technique, (2) the effect of GAC size on membrane fouling and adsorption capability of model foulants, (3) the potential fouling by GAC residues, and (4) the effect of GAC scouring on membrane integrity. This information can help us understand the behavior of GAC in the AFMBR and assist in choosing suitable GAC types, membrane materials, and membrane module designs for AFMBRs.

2. Materials and methods

2.1. GAC particles

Three types of GAC particles were used in this study. Their properties (provided by the suppliers) are summarized in Table 1 and their morphologies are shown in Fig. 1.

2.2. Model foulants

Bovine serum albumin (BSA, 100 mg/L, Sinopharm Chemical Reagent Co. Ltd, China), sodium alginate (SA, 100 mg/L, Hanawa Chemical, Japan), and humic acid (HA, 100 mg/L, Aldrich–Sigma, US) representative of proteins, polysaccharides, and humic substances, respectively, were mixed with bentonite (100 mg/L, Aldrich–Sigma, US) as the model foulant suspension (simulating the effluent of anaerobic bioreactor).

2.3. Direct observation of cake layer removal by GAC scouring

A cross-flow filtration module with a microscope was set up as previously reported [12]. A flat sheet Anopore membrane (0.2 μm) was used in this study. GAC was placed in the module channel (109 mm length × 34 mm width × 8 mm height) at the start of the test and the model foulant suspension was fed into the system (see Fig. S1 in supplementary data). The experiments were conducted at a flux of 80 $L/m^2 h$ (above the critical flux of about 40 $L/m^2 h$; in order to fasten cake layer formation) and a cross-flow rate of 0.02 m/s. For preliminary microscope observation, the module was positioned horizontally (GAC was settled

Table 1
Properties of the commercial GAC used in this study

Abbreviation in this study	GAC1	GAC2	GAC3
Brand	Norit	Norit	Norit
Origin	Lignite coal (acid wash)	Peat bog (untreated)	Peat bog (untreated)
Average particle diameter (mm)[a]	~0.42–0.85	~0.85–2.4	~2.4–4.6
Surface area (m^2/g)[a]	650	600–800	600–800

[a]Information obtained from product datasheets.

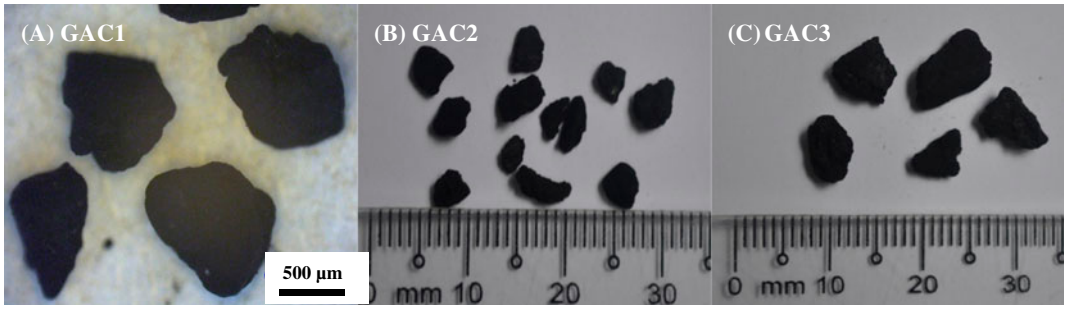

Fig. 1. Morphologies of GAC particles. Image (A) was taken by a microscope (×100 magnification, Keyence, Japan). Images (B) and (C) were taken by a Nikon camera (Japan).

inside the channel due to gravity, i.e. no GAC scouring). During the GAC souring stage, the module was aligned vertically to simulate the AFMBR (GAC was fluidized inside the channel). After a period of fluidization, the module was positioned horizontally again for microscope observation (Note: the same location of the membrane surface was observed by fixing the microscope plate holder). Transmembrane pressure (TMP) was recorded by a transducer (Core-Palmer, USA), which was connected to a computer equipped with Labview (National Instruments, US).

2.4. Membrane filtration setup

A bench-scale stirred dead-end filtration assay (Fig. 2) was set up to investigate the effect of activated carbon addition on membrane fouling and membrane integrity. Briefly, a virgin membrane (0.00125 m^2 of surface area) was put in a filtration cell. A magnetic stirrer bar (effective length of 26 mm) was installed in the filtration cell and located at 10 mm above the membrane surface. The rotation speed of the stirrer bar was fixed at ~150 rpm, which ensured GAC moved slowly across the membrane surface. The feed suspension was pumped into the filtration cell in order to maintain a constant water level in the filtration cell. The permeate flux (14 L/m^2 h, sub-critical flux) was maintained by controlling the flow rate of the permeate pump (Core-Palmer, US). TMP was recorded by a transducer (Core-Palmer, US), which was connected to a computer equipped with Labview (National Instruments, US).

Polyvinylidene fluoride (PVDF 0.1 μm, Merck Millipore, US) membranes, 100 mL of model foulant solution, and 0.4 g of GAC (equivalent to a loading of 320 g/m^2 membrane) were used to study the effect of GAC size on membrane fouling. Initially, the TMP of the clean membrane was measured. After each experiment, the membrane was taken from the filtration cell and the foulants were gently removed from the membrane surface using distilled water. Then the physically cleaned membrane was put into the filtration cell with distilled water and the TMP was recorded. The fouling resistance (R) was calculated by the equation: $R = \mathrm{TMP}/(\mu J)$, where μ is the permeate viscosity and J is permeate flux.

2.5. Adsorption kinetics of GAC

The experimental runs were carried out in batch mode with the same conditions as the filtration experiments. Each sample consists of a 100 mL of model mixture suspension, in contact with 0.4 g of PAC particles. At certain of time, 10 mL of solution was sampled and the total organic carbon (TOC) was measured by a TOC analyzer (Shimadzu, Japan) after being filtered by a 0.45-μm filter.

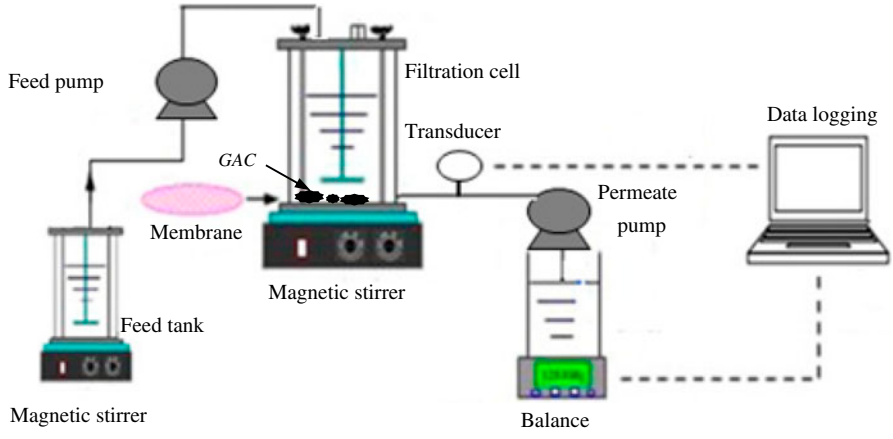

Fig. 2. A bench-scale stirred dead-end filtration setup.

2.6. Properties of released carbon particles from GAC

To estimate the release of carbon particles from GAC in the filtration experiment, 0.4 g of GAC was added into the filtration cell filled with model foulant suspension or distilled water (100 mL). The stirrer was rotated at a speed of ~150 rpm, but no filtration was performed. At a certain time interval, a sample (20 mL) was taken for analysis. The zeta potential was measured by a zetasizer (Malvern, UK) and the turbidity was determined by a Turbidity meter (Hach, USA). The pH was monitored by a pH meter (Mettler Toledo, Switzerland). The size distribution of released fine carbon particles was analyzed by a zetasizer (Malvern, UK).

2.7. Permeability, sodium alginate rejection, morphology of membranes after GAC scouring

Hydrophilic PVDF (0.22 μm, Merck Millipore, US) and cellulose acetate (CA, 0.2 μm, CEMS marketing Pte Ltd, Singapore) membranes were used in membrane integrity tests.

In the membrane integrity test, distilled water (100 mL) and activated carbon (0.4 g, equivalent to a loading of 320 g/m^2 membrane) were added into the filtration cell. Membrane permeability (P, L/m^2 h/kPa) was calculated as $P = \text{Flux}/\text{TMP}$. The averaged membrane permeability (over a period of 30 min) in the absence of GAC was calculated as P_0. After GAC scouring, the averaged permeability (over 30 min) was calculated as P_1. The membrane permeability increase rate was calculated as $[(P_1 - P_0)/P_0] \times 100\%$.

The sodium alginate rejection was another parameter used to indicate the membrane integrity. After membrane filtration with GAC was performed for 3 h, the GAC and distilled water was removed from the filtration cell. Then 100-mL sodium alginate (100 mg/L) was added into the filtration cell and the filtration was carried out at a flux of 14 LMH (sub-critical flux) for 30 min. The permeate was collected for TOC measurement by a TOC analyzer (Shimadzu, Japan).

An atomic force microscope (AFM, Park systems, Korea) was used to observe the roughness properties of the membranes before and after GAC abrasion. Tensile strength and tensile strain of the virgin membranes were measured using an extensometer (Zwick Roell, Germany).

3. Results and discussion

3.1. GAC removed cake layer from membrane surface by direct observation

Fig. 3 shows the images of the deposited foulants on the membrane before and after GAC1 fluidization captured by the camera equipped with the microscope. The cake layers were formed at a super-critical flux (80 LMH) after 15 min filtration (Fig. 3(A)). After that a short period (1 min) of GAC scouring was performed (the filtration was still conducted at 80 LMH).

Apparently, the relatively greater size foulant flocs were easily removed from the membrane after GAC scouring. At the same time, the TMP induced by the cake layer (TMPc) was reduced from 0.30 to 0.21 kPa. This illustrates that GAC scouring appears to reduce membrane fouling by removing the cake layers from the membrane.

3.2. GAC facilitated reduction of cake layer formation

In order to examine, whether the scouring effect of GAC was associated with the particle size, the

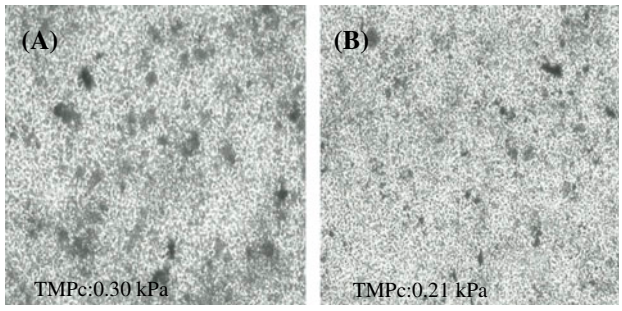

Fig. 3. Cake layer removal by GAC scouring via direct observation. The image (A) was taken after 15-min filtration (without GAC1 scouring) and then GAC1 fluidization was performed. The image (B) was taken after 1-min GAC1 fluidization.

membrane filtrations were performed at a flux of $14\,L/m^2\,h$ (sub-critical flux) in a stirring dead-end filtration cell for 16 h. Fig. 4 presents the resistances of the cake layer fouling and irreversible fouling when the GAC particles with different sizes were employed in the microfiltration.

After 16-h filtration, cake layer fouling contributed to more than 80% of the fouling in the absence/presence of GAC scouring, and was considered as the predominant fouling (Fig. 4). Compared with the total fouling resistance without GAC scouring (average of $0.98 \times 10^{12}\,m^{-1}$), the presence of GAC1, GAC2, and GAC3 particles lowered the total fouling resistance (average of 0.68×10^{12}, 0.59×10^{12}, and $0.58 \times 10^{12}\,m^{-1}$, respectively). In particular, the resistances of cake layers formed with GAC scouring (average of 0.62×10^{12}, 0.49×10^{12}, $0.45 \times 10^{12}\,m^{-1}$ for GAC1, GAC2, and GAC3, respectively) were much less than that without GAC scouring (average of $0.96 \times 10^{12}\,m^{-1}$). These results confirm that GAC scouring enhances membrane filtration performance by reduction of cake layer formation.

In addition, compared with smaller GAC1 particles, the presence of larger GAC2 and GAC3 particles showed slightly more benefit to membrane filtration. There was almost no obvious difference in cake layer resistance in the presence of GAC2 and GAC3 particles. This suggests that the enhancement of filtration performance by GAC scouring was little influenced by GAC size (within a range of 0.42–4.6 mm). Our findings are consistent with the observations of Noordman et al. [13] who noted that the mass transfer improvement by fluidized particles was a weak function of particle size (in the range 0.46–2 mm). On the other hand, the energy for fluidizing smaller GAC particles tends to be lower than fluidizing greater ones. Thus, it was suggested to use low density and smaller particles to promote energy saving in fluidized particle membrane filtration processes [13].

Interestingly, it was noted that the irreversible fouling resistances were consistently higher in the presence of GAC scouring than without GAC scouring (Fig. 4). On the one hand, GAC particles provide adsorptive removal of soluble foulants (to be described in Section 3.3) to potentially reduce irreversible fouling. On the other hand, the released fine particles from GAC during fluidization may block membrane pores or form a thin cake layer on the membrane (to be described in Section 3.4). These carbon foulants may not be readily removed by GAC abrasion, as a result, accelerating the irreversible fouling. This finding is consistent with our observation in Fig. 3 that small foulants were not easily dispatched from the membranes by GAC scouring.

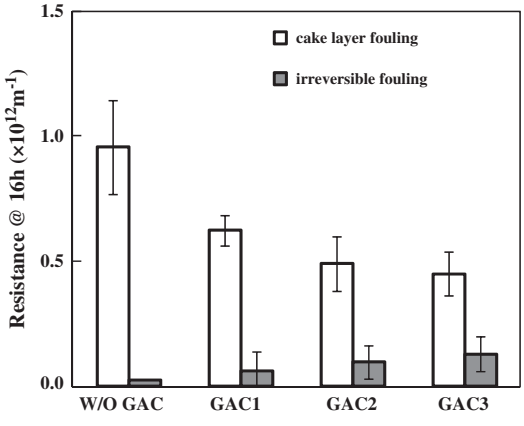

Fig. 4. Effect of GAC size on membrane fouling resistance.

3.3. GAC adsorbed the potential foulants

As activated carbon, GAC displayed adsorption capability. Fig. 5 shows the model solution adsorption kinetics of the GAC particles. Compared with the smaller sized GAC particles (GAC1), the larger sized GAC particles (GAC2 and GAC3) had better adsorption capability, presumably due to their greater active surface area (see Table 1).

It was also found that the addition of GAC to the model foulant suspension influenced the suspension properties (Fig. 6, the measurements were carried out after 2 h mixing). At the experimental temperature (25°C), the pH level of the model foulant suspension was around 7.1. The presence of GAC1 decreased pH level of the model foulant suspension to around 6.9.

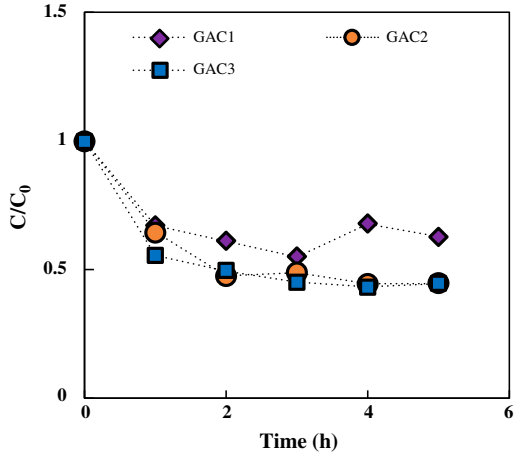

Fig. 5. Effect of GAC size on adsorption kinetics.

However, adding GAC2 and GAC3 to the model foulant suspension induced increases of pH values (pH of 8.4 and 8.3, respectively). The model foulant suspension contained highly negatively charged groups (i.e. zeta potential of −71.8 mV). An increasing trend of zeta potential of the model foulant suspension was noted after adding GAC particles (−61 ± 6, −64 ± 6, and −52 ± 5 mV for GAC1, GAC2, and GAC3, respectively). Possibly, the released fine carbon particles from GAC had positively charged surfaces, which performed neutralization with the model foulant suspension. The changes of the model foulant suspension characteristics are possibly related to the various origins and pretreatment methods of the GAC (Table 1).

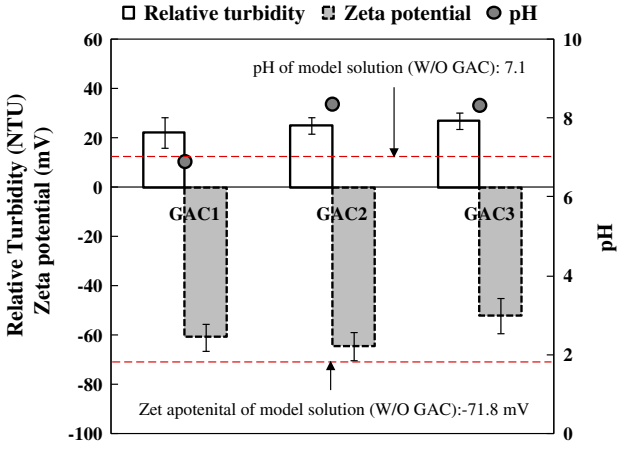

Fig. 6. The presence of GAC influenced the properties of model foulants in microfiltration. Relative turbidity is the difference between the turbidity of the model foulant suspension with GAC and the turbidity of the model foulant suspension W/O GAC.

Therefore, besides the intrinsic properties of the GAC affecting the GAC adsorption capability, the changes of model foulant suspension characteristics due to the presence of GAC were also a significant factor to influence adsorption kinetics of GAC.

3.4. GAC released fine carbon particles

In Sections 3.1–3.3, we have illustrated the positive roles of GAC particles in a hybrid GAC membrane filtration processes, namely, (1) GAC performed a "scouring membrane" role, accordingly, less cake formed on the membrane; (2) GAC displayed a capability to adsorb the potential foulants. However, even under a gentle shear rate, GAC could release fine particles, which would tend to adhere to the membrane surface. In addition, the direct interactions of GAC with the membrane inevitably cause "mechanical stress" on the membrane, which increases the risk of membrane damage. In Sections 3.4 and 3.5, we will discuss these two behaviors, which negatively influence membrane filtration.

Fig. 6 shows that the presence of GAC led to an increase in turbidity of the model foulant solution (20–30 NTU relative turbidity). This suggests that GAC released fine loosely attached carbon particles under such a shear force (induced by stirring). Within the experimental time (2 h), the amount of the released carbon particles was relatively independent of the GAC size.

The size distributions of the released fine carbon particles from different GAC particles were compared by mixing GAC with distilled water in the filtration cell under a stirring condition (~150 rpm). Fig. 7 indicates that the dominant size of the fine carbon particles from GAC1 and GAC2 was relatively larger than that from GAC3. In addition, the fine carbon particles released from GAC had a broad size range. It can be seen that a portion of them had comparable sizes with the membrane pore sizes, accordingly, appearing to invade and accumulate into the membrane volume. Optical microscope images (Fig. S3 in supplementary data) revealed the deposition of micro- and submicron-sized carbon particles on the membrane surface. This behavior could explain why the irreversible fouling increased when GAC particles were employed in the microfiltration process (Fig. 4).

Here, we would like to emphasize that the amount of deposition of the fine carbon particles on the membranes was dependent on the characteristics of the released carbon particles and the interaction potential between the released carbon particles and membranes (Fig. S3 in supplementary data).

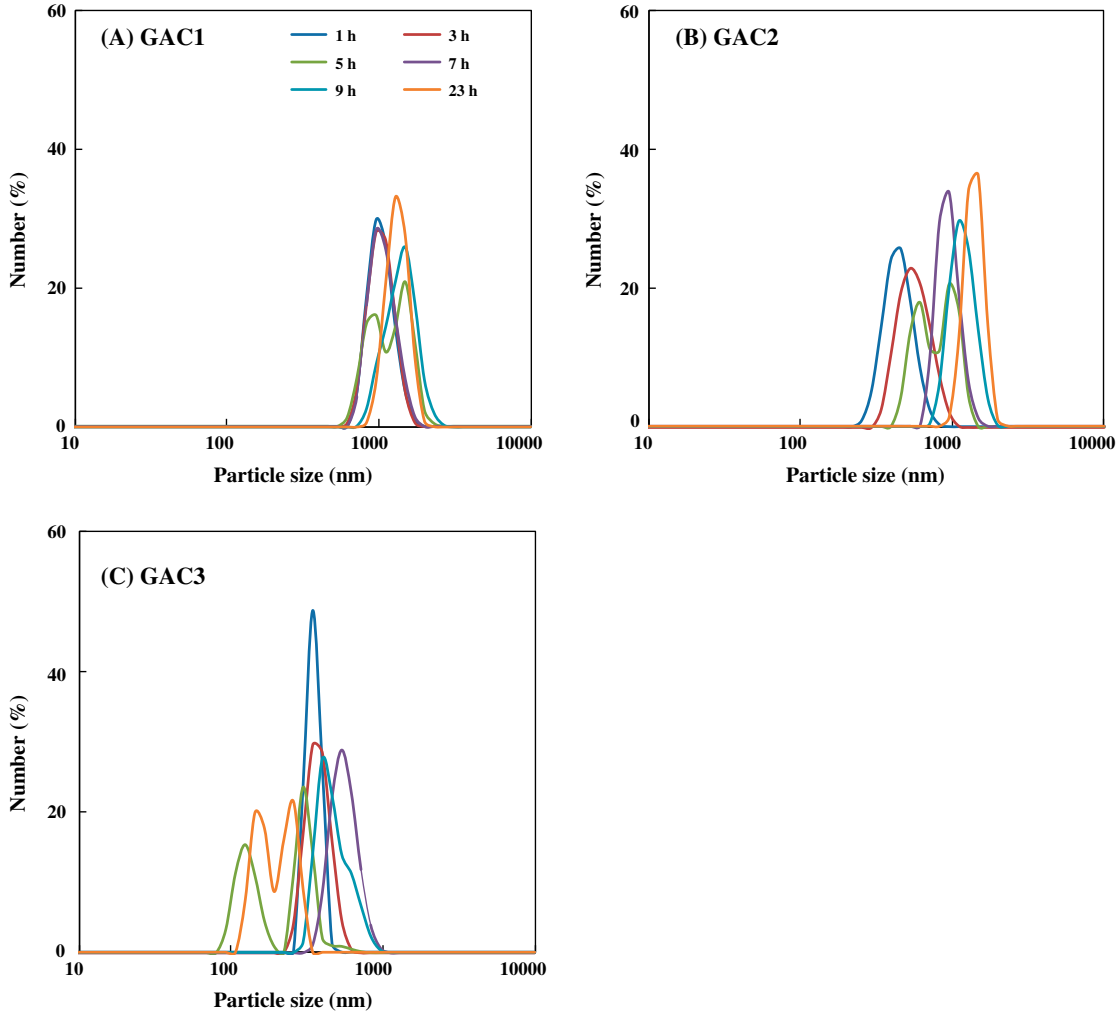

Fig. 7. Size distribution of released fine carbon particles from GAC.

3.5. GAC influenced membrane integrity

In this section, we compare the clean water permeability and sodium alginate rejection of the microfiltration membranes before and after GAC addition to test whether fluidized GAC particles influence membrane integrity. To evaluate the influences of GAC size and membrane material on the initial membrane integrity (i.e. the initial interactions of GAC with membranes) in the hybrid GAC microfiltration process, the maximum membrane clean water permeability increase rates within the first 3-h filtration were compared. Multi-replicate experiments ($n \geq 5$) were made and the averaged data are presented in Fig. 8(A). The deviations of the experimental data are relatively pronounced. This may be related with the wide ranges of the membrane pore size distributions (Fig. S2 in supplementary data) and irregular shapes of the tested GAC (Fig. 1).

After GAC2 addition into the microfiltration, the averaged clean water permeability of the CA membrane increased 29.1%, which was much higher than that of the PVDF membrane (9.3%) (T-test, p-value <0.05). In the presence of GAC1 and GAC3, the averaged clean water permeabilities of the CA membrane increased 12.5 and 20.3%, respectively, slightly more than those of the PVDF membrane (8.7 and 8.6%), but showing statistically insignificant differences (p-value >0.05) from the PVDF membrane. In addition, for each type of membrane, the effect of GAC size on membrane clean water permeability appeared to be less significant (p-value >0.05).

The increase in membrane clean water permeability implies that GAC influenced membrane integrity. SEM images further confirmed that the interactions of GAC with membrane surface led to the loss of membrane integrity (data not shown). Various possible

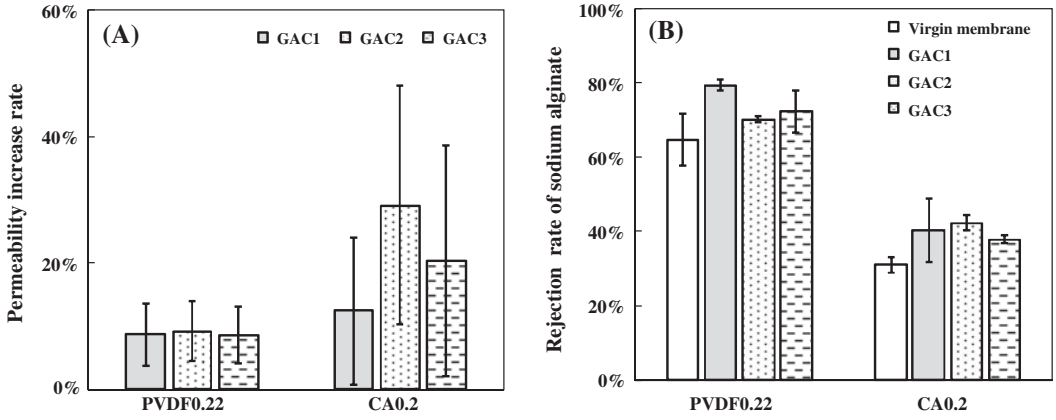

Fig. 8. Membrane permeability increase rate (A) and sodium alginate rejection (B) by the virgin membranes and the membranes after GAC abrasion for 3 h.

changes in membrane morphology were observed, for example, changes in membrane pore configurations, enlargement of the existing membrane pores, and separation of the membrane surface layer from the support layer. Whether the presence of GAC facilitated the creation of new pores on the membranes was not easily identified by the SEM images. AFM images (Fig. 9) also show that GAC scouring tended to change the morphology of the membrane.

The membrane roughness is presented in Fig. 10 from analysis of AFM images. There was an almost unnoticeable difference in the roughness of the PVDF membranes in the absence or presence of GAC particles in the microfiltration. However, GAC abrasion led to significant changes of CA membrane roughness. As discussed, GAC abrasion as well as the deposition of released fine carbon particles on the membrane could influence membrane surface characteristics. Thus, the changes in membrane roughness after GAC scouring are attributed to the combined effects of the membrane integrity loss and fine carbon particle fouling. Compared with the CA membrane, the PVDF membrane had less membrane integrity loss (i.e. less membrane permeability increase) after GAC scouring and more interactions with the released fine carbon particles (Fig. S3 in supplementary data). As a result, less roughness changes of the PVDF membrane were expected compared with those of the CA membrane.

It will be recalled that the clean water permeability increase rates of the PVDF membrane after GAC abrasion was lower than those of the CA membrane (Fig. 8(A)). Generally, tensile strength and tensile strain are the parameters used to evaluate membrane strength and elongation properties, respectively. Fig. 11 indicates that CA membranes were stronger than PVDF membrane, but they had poor elongation and were characterized as brittle. The three types of GAC had irregular configurations and sharp edges (Fig. 1), which could create strong abrasive forces when the sharp edges interacted with membranes. The PVDF membrane, having excellent resilience, appeared to tolerate the GAC-induced shear force compared with CA membranes.

Fig. 8(B) shows the sodium alginate rejections of the virgin membranes and the membranes after GAC abrasion for 3 h. Compared with the CA virgin membranes, the PVDF virgin membrane had a relatively higher rejection ($64.8 \pm 7.0\%$ vs. $31.0 \pm 2.1\%$). Interestingly, the presence of GAC in microfiltration improved the rejection (averagely 7–9%) and the increase ratio was independent of GAC sizes.

In recent research work, Meier observed that PAC particles could damage nanofiltration membranes functional layer by observing an increase of permeate flux and a decrease in $MgSO_4$ solution rejection with time [14]. In contrast to Meier's observations, we have found that some membrane integrity was lost due to GAC scouring (membrane permeability increases), but sodium alginate rejection rates were also increased. As mentioned in the Section 3.4, the micro- and nano-sized fine carbon particles could release from GAC, which tend to deposit on the membrane surface or fill into membrane pores during filtration processes. Possibly, the carbon foulants tended to modify the membrane surface characteristics and membrane pore size distribution, which facilitated the rejection of sodium alginate.

Therefore, in the hybrid GAC microfiltration process, GAC concurrently performed two roles which

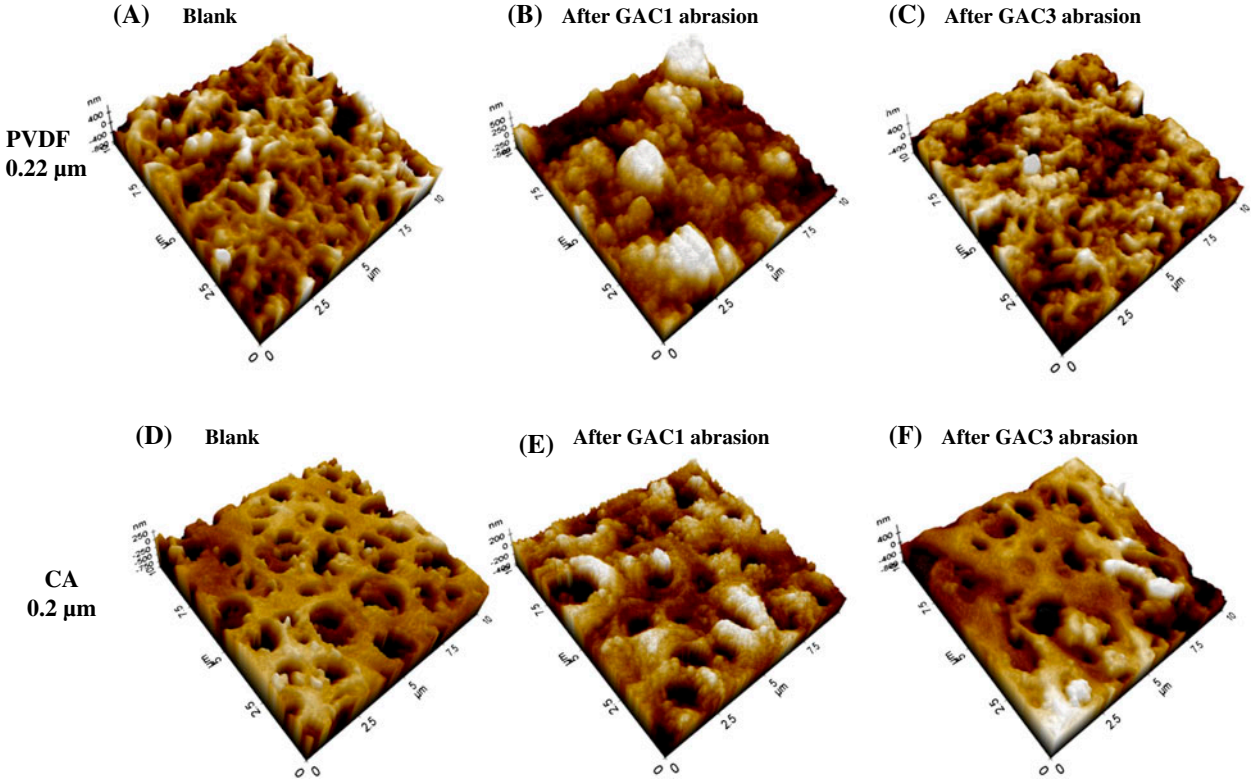

Fig. 9. AFM images of PVDF and CA membranes before and after GAC abrasion.

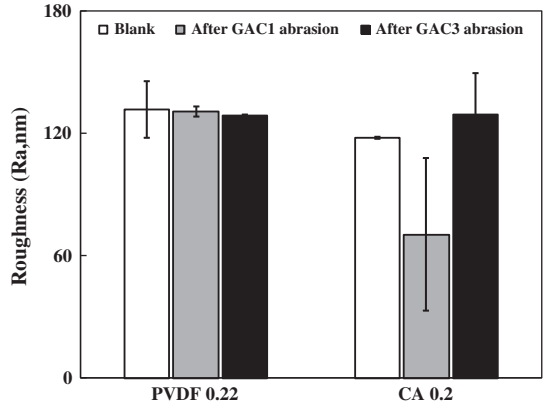

Fig. 10. Roughness of PVDF and CA membranes before and after GAC abrasion.

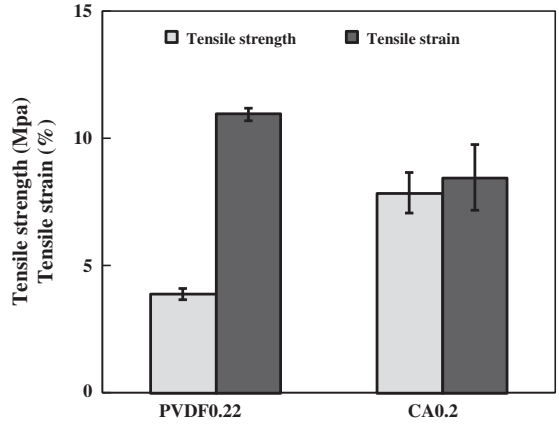

Fig. 11. Membrane mechanical properties.

were mentioned by Meier [14]. That is, (1) the mechanical effect of GAC induces loss of membrane integrity, as a result, increasing membrane permeability and decrease rejection; (2) the released fine carbon particles deposit on the membrane (i.e. as "secondary membrane"), block or narrow membrane pores (i.e. reducing nominal membrane pore size) to decrease membrane permeability and increase rejection. On the other hand, the fine carbon cake layers may lessen the direct interactions of GAC with the primary membrane, protecting the membrane from further damage. The combined effects of the two counteracting GAC roles determined the membrane permeability and rejection. Further work may be required to confirm this hypothesis.

4. Conclusions

In this study, we employed bench membrane filtration tests to investigate GAC potential roles in the AFMBR. By direct observation through the membrane, we found that GAC scouring could remove the greater size foulants from the membrane surface. The reduction of cake layer resistance by GAC abrasion was weakly associated with GAC size. In addition, the addition of GAC in the model foulant solution tended to influence its pH and zeta potential. Thus, the GAC adsorption kinetics was related with the GAC origin and pretreatment rather than its particle size. With addition of GAC in microfiltration, both the membrane permeability and sodium alginate rejection increased. Membrane morphology changes after GAC abrasion was observed by SEM and AFM images, predominantly contributing to membrane permeability increase. On the other hand, under stirring conditions, GAC released fine carbon particles, which may have blocked/narrowed pores and formed thin cake layers facilitating increases in rejection. Membrane integrity loss was determined less by GAC size, but rather by the membrane material properties. Compared with the CA membrane, the PVDF membrane with good elongation properties displayed great tolerance to GAC abrasion. There are several parameters, such as membrane materials and GAC stability, which need to be carefully evaluated in order to achieve optimal performance of the AFMBR.

Supplementary material

The supplementary material for this paper is available online at http://dx.doi.10.1080/19443994.2014.943057.

Acknowledgments

The authors thank Jillinda Toh, Steven Limbra, Cui Xian Liou, Yuanyuan Wang, and Alvin Chew for their kind help. This research grant is supported by the Singapore National Research Foundation under its Environmental & Water Technologies Strategic Research Programme and administered by the Environment & Water Industry Programme Office (EWI) of the PUB. The EDB is also acknowledged for funding the Singapore Membrane Technology Centre (SMTC), Nanyang Technological University.

References

[1] D.C. Stuckey, Recent developments in anaerobic membrane reactors, Bioresour. Technol. 122 (2012) 137–148.
[2] J. Kim, K. Kim, H. Ye, E. Lee, C. Shin, P.L. McCarty, J. Bae, Anaerobic fluidized bed membrane bioreactor for wastewater treatment, Environ. Sci. Technol. 45 (2011) 576–581.
[3] R. Yoo, J. Kim, P.L. McCarty, J. Bae, Anaerobic treatment of municipal wastewater with a staged anaerobic fluidized membrane bioreactor (SAF-MBR) system, Bioresour. Technol. 120 (2012) 133–139.
[4] P.L. McCarty, J. Bae, J. Kim, Domestic wastewater treatment as a net energy producer-can this be achieved? Environ. Sci. Technol. 45 (2011) 7100–7106.
[5] X. Huang, C.H. Wei, K.C. Yu, Mechanism of membrane fouling control by suspended carriers in a submerged membrane bioreactor, J. Membr. Sci. 309 (2008) 7–16.
[6] M.A.H. Johir, R. Aryal, S. Vigneswaran, J. Kandasamy, A. Grasmick, Influence of supporting media in suspension on membrane fouling reduction in submerged membrane bioreactor (SMBR), J. Membr. Sci. 374 (2011) 121–128.
[7] C.A. Ng, D. Sun, J.S. Zhang, B. Wu, A.G. Fane, Mechanisms of fouling control in membrane bioreactors by the addition of powdered activated carbon, Sep. Sci. Technol. 45 (2010) 873–889.
[8] C.H. Wei, X. Huang, C.W. Wang, X.H. Wen, Effect of a suspended carrier on membrane fouling in a submerged membrane bioreactor, Water Sci. Technol. 53 (2006) 211–220.
[9] C.-F. Lin, Y.-J. Huang, O.J. Hao, Ultrafiltration processes for removing humic substances: Effect of molecular weight fractions and PAC treatment, Water Res. 33 (1999) 1252–1264.
[10] C.-W. Li, Y.-S. Chen, Fouling of UF membrane by humic substance: Effects of molecular weight and powder-activated carbon (PAC) pre-treatment, Desalination 170 (2004) 59–67.
[11] B. Siembida, P. Cornel, S. Krause, B. Zimmermann, Effect of mechanical cleaning with granular material on the permeability of submerged membranes in the MBR process, Water Res. 44 (2010) 4037–4046.
[12] Y. Zhang, A. Fane, A. Law, Critical flux and particle deposition of bidisperse suspensions during crossflow microfiltration, J. Membr. Sci. 282 (2006) 189–197.
[13] T.R. Noordman, A. de Jonge, J.A. Wesselingh, W. Bel, M. Dekker, E. Voorde, S.D. Grijpma, Application of fluidised particles as turbulence promoters in ultrafiltration, J. Membr. Sci. 208 (2002) 157–169.
[14] J. Meier, Mechanical influence of PAC particles on membrane processes, J. Membr. Sci. 360 (2010) 404–409.